RegCM Version 3.0
User's Guide

Physics of Weather and Climate Group
International Centre for Theoretical Physics

MIRAMARE–TRIESTE
February 2004

Written by Nellie Elguindi, Xunqiang Bi, Filippo Giorgi, Badrinath Nagarajan, Jeremy Pal, and Fabien Solmon

Abstract

As one of the main aims of the ICTP is to foster the growth of advanced studies and research in developing countries, the main purpose of this Regional Climate Model (RegCM) Tutorial Class Notes is to give model users a guide to learn the whole RegCM Model System.

The RegCM Tutorial Class is offered as a part of extended hands-on lab sessions during a series of Workshops organized by the Physics of Weather and Climate (PWC) group at the Abdus Salam International Centre for Theoretical Physics (ICTP).

RegCM was originally developed at the National Center for Atmospheric Research (NCAR) and has been mostly applied to studies of regional climate and seasonal predictability around the world. The workshop participants are welcome to use RegCM for regional climate simulation over different areas of interest. The RegCM is available on the World Wide Web at
http://www.ictp.trieste.it/~pubregcm/RegCM3.

Contents

1 Introduction **4**
- 1.1 History . . . 4
- 1.2 The RegCM Model Horizontal and Vertical Grid . . . 6
- 1.3 Map Projections and Map-Scale Factors . . . 8

2 Model Description **9**
- 2.1 Dynamics . . . 9
- 2.2 Physics . . . 11
  - 2.2.1 Radiation Scheme . . . 11
  - 2.2.2 Land Surface Model . . . 11
  - 2.2.3 Planetary Boundary Layer Scheme . . . 12
  - 2.2.4 Convective Precipitation Schemes . . . 12
  - 2.2.5 Large-Scale Precipitation Scheme . . . 17
  - 2.2.6 Ocean flux Parameterization . . . 18
  - 2.2.7 Pressure Gradient Scheme . . . 18
  - 2.2.8 Lake Model . . . 18
  - 2.2.9 Tracer Model . . . 19

3 Pre-Processing **20**
- 3.1 Terrain . . . 21
- 3.2 ICBC . . . 23
  - 3.2.1 Sea surface temperature . . . 23
  - 3.2.2 Initial and Boundary Conditions . . . 23

4 RegCM **25**

5 Post-processing **26**

6 Practice Run **27**
- 6.1 Getting the model code and data . . . 27
- 6.2 Pre-processing . . . 27
  - 6.2.1 Setting up the domain . . . 27
  - 6.2.2 ICBC . . . 29
- 6.3 Running the Model . . . 29
  - 6.3.1 Restarting the model . . . 30

List of Figures

1 Schematic representation of the vertical structure of the model. This example is for 14 vertical layers. Dashed lines denote half-sigma levels, solid lines denote full-sigma levels. (Adapted from the PSU/NCAR Mesoscale Modeling System Tutorial Class Notes and User's Guide.) 6
2 Schematic representation showing the horizontal Arakawa B-grid staggering of the dot and cross grid points. 7

List of Tables

1 Land Cover/Vegetation classes 21
2 BATS vegetation/land-cover 22
3 List of variables defined in *domain.param* file. 31
4 List of output variables from Terrain (DOMAIN) 32
5 List of variables in *ICBCYYYYMMDDHH* files 32
6 List of restart, timestep, and output parameters defined in *regcm.in* file. . . 33
7 List of physic options in *regcm.in* file. 34
8 List of output variables from atmosphere 35
9 List of output variables from surface model 35
10 List of output variables from radiation model 36
11 List of output variables from tracer model 36
12 List of variables to be modified in *domain.param* file. 37
13 List of variables to be modified in *regcm.in* file. 37
14 List of variables to be modified in *regcm.in* file. 38

1 Introduction

1.1 History

The idea that limited area models (LAMs) could be used for regional studies was originally proposed by Dickinson et al. (1989) and Giorgi (1990b). This idea was based on the concept of one way nesting, in which large scale meteorological fields from general circulation model (GCM) runs provide initial and time-dependent meteorological lateral boundary conditions (LBC) for high resolution regional climate model (RCM) simulations, with no feedback from the RCM to the driving GCM.

The first generation NCAR RegCM was built upon the National Center for Atmospheric Research-Pennsylvania State University (NCAR-PSU) Mesoscale Model version MM4 in the late 1980s (Dickinson et al. 1989, Giorgi 1989). The dynamical component of the model originated from that of the MM4, which is a compressible, finite difference model with hydrostatic balance and vertical σ-coordinates. Later the use of a split-explicit time integration scheme was added along with an algorithm for reducing horizontal diffusion in the presence of steep topographical gradients (Giorgi et al. 1993a, Giorgi et al. 1993b). As a result the dynamical core of the RegCM is similar to that of the hydrostatic version of MM5 (Grell et al. 1994a).

For application of the MM4 to climate studies, a number of physics parameterizations were replaced, mostly in the areas of radiative transfer and land surface physics, which led to the first generation RegCM (Dickinson et al. 1989, Giorgi 1990b). The first generation RegCM included the Biosphere-Atmosphere Transfer Scheme, BATS, (Dickinson et al. 1986) for surface process representation, the radiative transfer scheme of the NCAR Community Climate Model (CCM) version CCM1, a medium resolution local planetary boundary layer scheme, the Kuo-type cumulus convection scheme of (Anthes 1977) and the explicit moisture scheme of (Hsie et al. 1984).

A first major upgrade of the model physics and numerical schemes was documented by (Giorgi et al. 1993a, Giorgi et al. 1993b), and resulted in a second generation RegCM, hereafter referred to as RegCM2. The physics of RegCM2 was based on that of the NCAR CCM2 (Hack et al. 1993), and the mesoscale model MM5 (Grell et al. 1994a). In particular, the CCM2 radiative transfer package (Briegleb 1992) was used for radiation calculations, the non local boundary layer scheme of (Holtslag et al. 1990) replaced the older local scheme, the mass flux cumulus cloud scheme of (Grell 1993) was added as an option, and the latest version of BATS1E (Dickinson et al. 1993) was included in the model.

In the last few years, some new physics schemes have become available for use in the RegCM, mostly based on physics schemes of the latest version of the CCM, CCM3 (Kiehl et al. 1996). First, the CCM2 radiative transfer package has been replaced by that of the CCM3. In the CCM2 package, the effects of H_2O, O_3, O_2, CO_2 and clouds were accounted for. Solar radiative transfer was treated with a δ-Eddington approach and cloud radiation depended on three cloud parameters, the cloud fractional cover, the cloud liquid water content, and the cloud effective droplet radius. The CCM3 scheme retains the same structure as that of the CCM2, but it includes new features such as the effect of additional greenhouse gases ($NO_2, CH_4, CFCs$), atmospheric aerosols, and cloud ice.

The other primary changes are in the areas of cloud and precipitation processes. The original explicit moisture scheme of (Hsie et al. 1984) has been substituted with a simpli-

fied version of it. This is because the original scheme was computationally too expensive to be run in climate mode. In the simplified scheme only a prognostic equation for cloud water is included, which accounts for cloud water formation, advection and mixing by turbulence, re-evaporation in sub-saturated conditions, and conversion into rain via a bulk autoconversion term. The main novelty of this scheme does not reside of course in the simplistic microphysics, but in the fact that the prognosed cloud water variable is directly used in the cloud radiation calculations. In the previous versions of the model, cloud water variables for radiation calculations were diagnosed in terms of the local relative humidity. This new feature adds a very important and far reaching element of interaction between the simulated hydrologic cycle and energy budget calculations.

Finally, an important aspect of model development was the inclusion of a stretched grid model configuration, by which the model horizontal resolution is relatively coarse in the lateral buffer zone and increases towards the interior of the domain. Preliminary experiments using an adiabatic version of the model in stretched grid mode are presented by (Qian et al. 1999). However, the stretched grid option is not available with the new RegCM3 version. Other new features in the RegCM include improvements in the coupled lake model (Small et al. 1999) and the incorporation of a tracer model with capability of radiative interactions (Qian et al. 1999).

There have been several improvements and additions to the newest version of the model, RegCM3, which will be released at this workshop. Changes in the model physics include a new large-scale cloud and precipitation scheme which accounts for the subgrid-scale variability of clouds (Pal et al. 2000), new parameterizations for ocean surface fluxes (Zeng et al. 1998), and a cumulus convection scheme (Betts 1986). Also new in the model is a mosaic-type parameterization of subgrid-scale heterogeneity in topography and land use (Giorgi et al. 2003b), however, this scheme is not included in the version released for the workshop but will soon be available.

Other improvements in RegCM3 involve the input data. The USGS Global Land Cover Characterization and Global 30 Arc-Second Elevation datasets are now used to create the terrain files. In addition, NCEP and ECMWF global reanalysis datasets are used for the intial and boundary conditions.

Lastly, improvements in the user-friendliness of the model have been made. New scripts have been included which make running the programs easier. Also, a new website has been developed where users can freely download the entire RegCM system, as well as all of the input data necessary for a simulation.

The whole released RegCM modeling system is composed by four components: Terrain, ICBC, RegCM, and Postprocessor. Terrain and ICBC are the two components of RegCM preprocessor. Terrestrial variables (include elevation, landuse and sea surface temperature) and three-dimensional isobaric meteorological data are horizontally interpolated from a latitude-longitude mesh to a high-resolution domain on either a Rotated (and Normal) Mercator, Lambert Conformal, or Polar Stereographic projection. Vertical interpolation from pressure levels to the σ coordinate system of RegCM is also performed. σ surfaces near the ground closely follow the terrain, and the higher-level σ surfaces tend to approximate isobaric surfaces.

Since the vertical and horizontal resolution and domain size can vary, the modeling package programs employ parameterized dimensions requiring a variable amount of core memory, and the requisite hard-disk storage amount is varied accordingly.

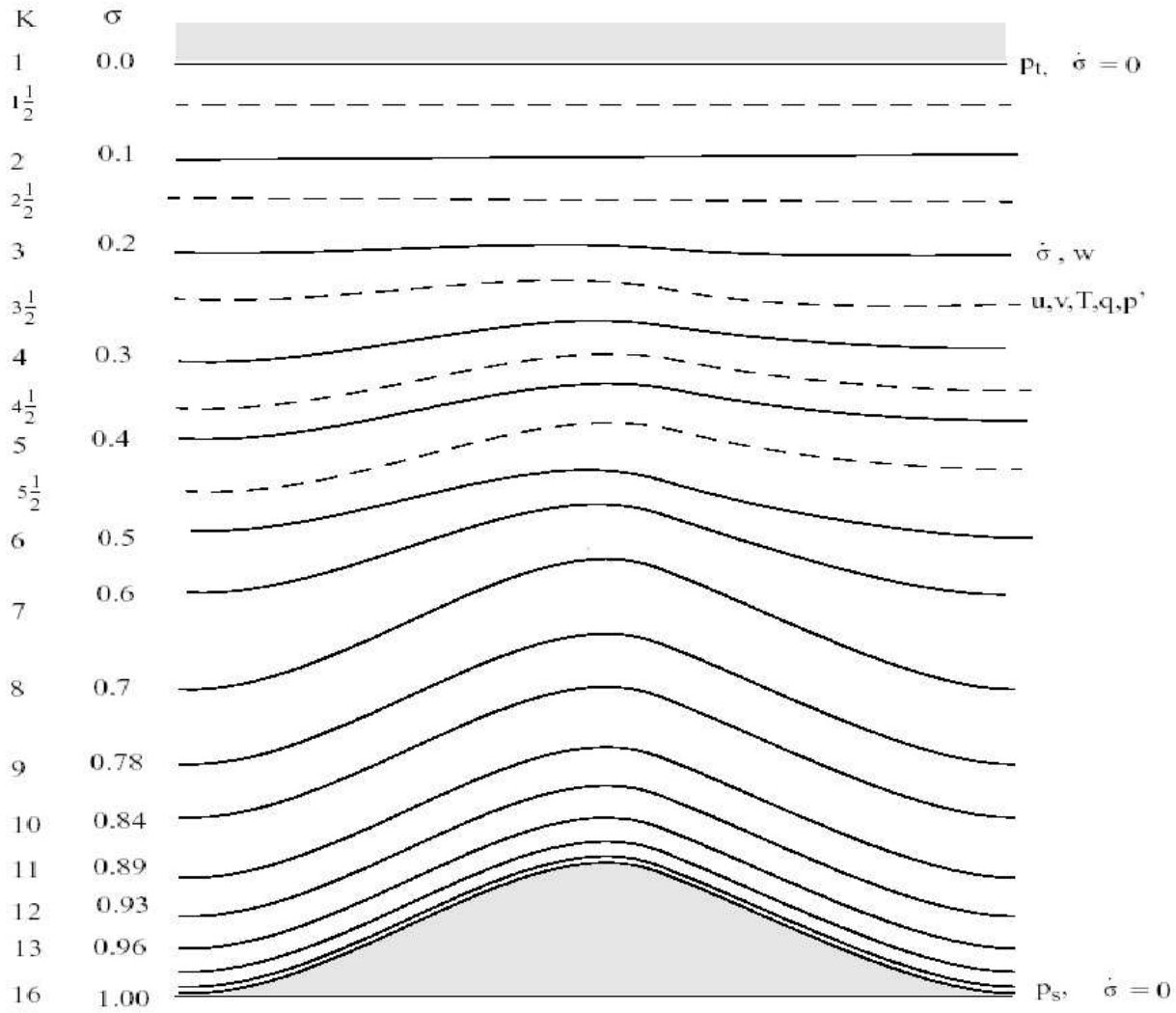

Figure 1: Schematic representation of the vertical structure of the model. This example is for 14 vertical layers. Dashed lines denote half-sigma levels, solid lines denote full-sigma levels. (Adapted from the PSU/NCAR Mesoscale Modeling System Tutorial Class Notes and User's Guide.)

1.2 The RegCM Model Horizontal and Vertical Grid

It is useful to first introduce the model's grid configuration. The modeling system usually gets and analyzes its data on pressure surfaces, but these have to be interpolated to the model's vertical coordinate before input to the model. The vertical coordinate is terrain following (Figure 1) meaning that the lower grid levels follow the terrain while the upper surface is flatter. Intermediate levels progressively flatten as the pressure decreases toward the top of the model. A dimensionless σ coordinate is used to define the model levels where p is the pressure, p_t is a specified constant top pressure, p_s is the surface pressure.

$$\sigma = \frac{(p - p_t)}{(p_s - p_t)} \tag{1}$$

It can be seen from the equation and Figure 1 that σ is zero at the top and one at the surface, and each model level is defined by a value of σ. The model vertical resolution is

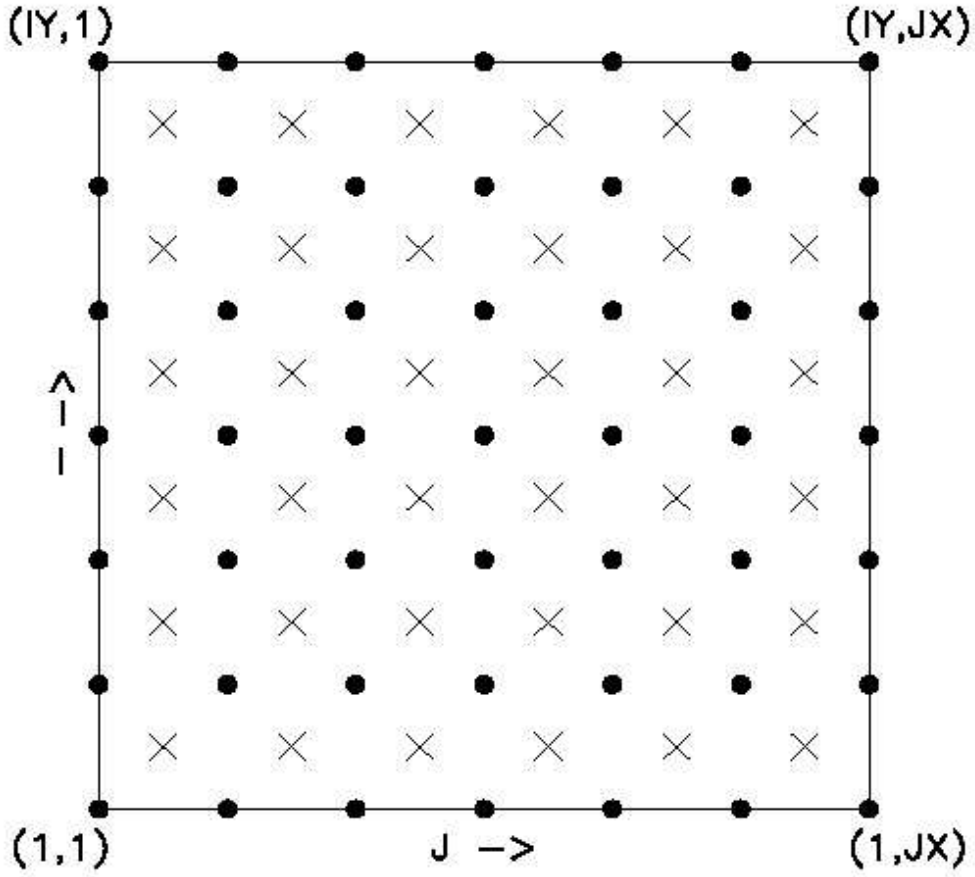

Figure 2: Schematic representation showing the horizontal Arakawa B-grid staggering of the dot and cross grid points.

defined by a list of values between zero and one that do not necessarily have to be evenly spaced. Commonly the resolution in the boundary layer is much finer than above, and the number of levels may vary upon the user demand.

The horizontal grid has an Arakawa-Lamb B-staggering of the velocity variables with respect to the scalar variables. This is shown in Figure 2 where it can be seen that the scalars (T, q, p, etc) are defined at the center of the grid box, while the eastward (u) and northward (v) velocity components are collocated at the corners. The center points of grid squares will be referred to as cross points, and the corner points are dot points. Hence horizontal velocity is defined at dot points. Data is input to the model, the preprocessors do the necessary interpolation to assure consistency with the grid.

All the above variables are defined in the middle of each model vertical layer, referred to as half-levels and represented by the dashed lines in Figure 1. Vertical velocity is carried at the full levels (solid lines). In defining the sigma levels it is the full levels that are listed, including levels at $\sigma = 0$ and 1. The number of model layers is therefore always one less than the number of full sigma levels.

The finite differencing in the model is, of course, crucially dependent upon the grid staggering wherever gradients or averaging are represent terms in the equation.

1.3 Map Projections and Map-Scale Factors

The modeling system has a choice of four map projections. Lambert Conformal is suitable for mid-latitudes, Polar Stereographic for high latitudes, Normal Mercator for low latitudes, and Rotated Mercator for extra choice. The x and y directions in the model do not correspond to west-east and north-south except for the Normal Mercator projection, and therefore the observed wind generally has to be rotated to the model grid, and the model u and v components need to be rotated before comparison with observations. These transformations are accounted for in the model pre-processors that provide data on the model grid, and in the post-processors. The map scale factor, m, is defined by

m = (distance on grid) / (actual distance on earth)

and its value is usually close to one, varying with latitude. The projections in the model preserve the shape of small areas, so that dx=dy everywhere, but the grid length varies across the domain to allow a representation of a spherical surface on a plane surface. Map-scale factors need to be accounted for in the model equations wherever horizontal gradients are used.

2 Model Description

2.1 Dynamics

The model dynamic equations and numerical discretization are described by (Grell et al. 1994a).

Horizontal Momentum Equations

$$\frac{\partial p^* u}{\partial t} = -m^2 \left(\frac{\partial p^* uu/m}{\partial x} + \frac{\partial p^* vu/m}{\partial y} \right) - \frac{\partial p^* u\dot{\sigma}}{\partial \sigma}$$
$$-mp^* \left[\frac{RT_v}{(p^* + p_t/\sigma)} \frac{\partial p^*}{\partial x} + \frac{\partial \phi}{\partial x} \right] + fp^* v + F_H u + F_V u, \tag{2}$$

$$\frac{\partial p^* v}{\partial t} = -m^2 \left(\frac{\partial p^* uv/m}{\partial x} + \frac{\partial p^* vv/m}{\partial y} \right) - \frac{\partial p^* v\dot{\sigma}}{\partial \sigma}$$
$$-mp^* \left[\frac{RT_v}{(p^* + p_t/\sigma)} \frac{\partial p^*}{\partial y} + \frac{\partial \phi}{\partial y} \right] + fp^* u + F_H v + F_V v, \tag{3}$$

where u and v are the eastward and northward components of velocity, T_v is virtual temperature, ϕ is geopotential height, f is the coriolis parameter, R is the gas constant for dry air, m is the map scale factor for either the Polar Stereographic, Lambert Conformal, or Mercator map projections, $\dot{\sigma} = \frac{d\sigma}{dt}$, and F_H and F_V represent the effects of horizontal and vertical diffusion, and $p^* = p_s - p_t$.

Continuity and Sigmadot ($\dot{\sigma}$) Equations

$$\frac{\partial p^*}{\partial t} = -m^2 \left(\frac{\partial p^* u/m}{\partial x} + \frac{\partial p^* v/m}{\partial y} \right) - \frac{\partial p^* \dot{\sigma}}{\partial \sigma}. \tag{4}$$

The vertical integral of Equation 4 is used to compute the temporal variation of the surface pressure in the model,

$$\frac{\partial p^*}{\partial t} = -m^2 \int_0^1 \left(\frac{\partial p^* u/m}{\partial x} + \frac{\partial p^* v/m}{\partial y} \right) d\sigma. \tag{5}$$

After calculation of the surface-pressure tendency $\frac{\partial p^*}{\partial t}$, the vertical velocity in sigma coordinates ($\dot{\sigma}$) is computed at each level in the model from the vertical integral of Equation 4.

$$\dot{\sigma} = -\frac{1}{p^*} \int_0^\sigma \left[\frac{\partial p^*}{\partial t} + m^2 \left(\frac{\partial p^* u/m}{\partial x} + \frac{\partial p^* v/m}{\partial y} \right) \right] d\sigma\prime, \tag{6}$$

where $\sigma\prime$ is a dummy variable of integration and $\dot{\sigma}(\sigma = 0) = 0$.

Thermodynamic Equation and Equation for Omega (ω)
The thermodynamic equation is

$$\frac{\partial p^* T}{\partial t} = -m^2 \left(\frac{\partial p^* uT/m}{\partial x} + \frac{\partial p^* vT/m}{\partial y} \right) - \frac{\partial p^* T\dot{\sigma}}{\partial \sigma} + \tag{7}$$

$$\frac{RT_v\omega}{c_{pm}(\sigma + P_t/p_{ast})} + \frac{p^* Q}{c_{pm}} + F_H T + F_V T, \tag{8}$$

where c_{pm} is the specific heat for moist air at constant pressure, Q is the diabatic heating, $F_H T$ represents the effect of horizontal diffusion, $F_V T$ represents the effect of vertical mixing and dry convective adjustment, and ω is

$$\omega = p^*\dot{\sigma} + \sigma \frac{dp^*}{dt}, \tag{9}$$

where,

$$\frac{dp^*}{dt} = \frac{\partial p^*}{\partial t} + m \left(u \frac{\partial p^*}{\partial x} + v \frac{\partial p^*}{\partial y} \right). \tag{10}$$

The expression for $c_{pm} = c_p(1 + 0.8q_v)$,
where c_p is the specific heat at constant pressure for dry air and q_v is the mixing ratio of water vapor.

Hydrostatic Equation
The hydrostatic equation is used to compute the geopotential heights from the virtual temperature T_v,

$$\frac{\partial \phi}{\partial ln(\sigma + p_t/p^*)} = -RT_v \left[1 + \frac{q_c + q_r}{1 + q_v} \right]^{-1}, \tag{11}$$

where $T_v = T(1 + 0.608q_v)$, q_v, q_c, and q_r are the water vapor, cloud water or ice, and rain water or snow, mixing ratios.

2.2 Physics

2.2.1 Radiation Scheme

RegCM3 uses the radiation scheme of the NCAR CCM3, which is described in (Kiehl et al. 1996). Briefly, the solar component, which accounts for the effect of O_3, H_2O, CO_2, and O_2, follows the δ-Eddington approximation of (Kiehl et al. 1996). It includes 18 spectral intervals from 0.2 to 5 μm. The cloud scattering and absorption parameterization follow that of (Slingo 1989), whereby the optical properties of the cloud droplets (extinction optical depth, single scattering albedo, and asymmetry parameter) are expressed in terms of the cloud liquid water content and an effective droplet radius . When cumulus clouds are formed, the gridpoint fractional cloud cover is such that the total cover for the column extending from the model-computed cloud-base level to the cloud-top level (calculated assuming random overlap) is a function of horizontal gridpoint spacing. The thickness of the cloud layer is assumed to be equal to that of the model layer, and a different cloud water content is specified for middle and low clouds.

2.2.2 Land Surface Model

The surface physics are performed using BATS1E (Biosphere-Atmosphere Transfer Scheme) which is described in detail by (Dickinson et al. 1993). BATS is a state of the art surface package designed to describe the role of vegetation and interactive soil moisture in modifying the surface-atmosphere exchanges of momentum, energy, and water vapor. The model has a vegetation layer, a snow layer, a surface soil layer, 10 cm thick, or root zone layer, 1-2 m thick, and a third deep soil layer 3 m thick. Prognostic equations are solved for the soil layer temperatures using a generalization of the force-restore method of (Deardoff 1978). The temperature of the canopy and canopy foilage is calculated diagnostically via an energy balance formulation including sensible, radiative, and latent heat fluxes.

The soil hydrology calculations include predictive equations for the water content of the soil layers. These equations account for precipitation, snowmelt, canopy foiliage drip, evapotranspiration, surface runoff, infiltration below the root zone, and diffusive exchange of water between soil layers. The soil water movement formulation is obtained from a fit to results from a high-resolution soil model (*Climate Processes and Climate Sensitivity* 1984) and the surface runoff rates are expressed as functions of the precipitation rates and the degree of soil water saturation. Snow depth is prognostically calculated from snowfall, snowmelt, and sublimation. Precipitation is assumed to fall in the form of snow if the temperature of the lowest model level is below 271 K.

Sensible heat, water vapor, and momentum fluxes at the surface are calculated using a standard surface drag coefficient formulation based on surface-layer similarity theory. The drag coefficient depends on the surface roughness length and on the atmospheric stability in the surface layer. The surface evapotranspiration rates depend on the availability of soil water. BATS has 20 vegetation types (Table 2; soil textures ranging from coarse (sand), to intermediate (loam), to fine (clay); and different soil colors (light to dark) for the soil albedo calculations. These are described in (Dickinson et al. 1986).

2.2.3 Planetary Boundary Layer Scheme

The planetary boundary layer scheme, developed by (Holtslag et al. 1990), is based on a nonlocal diffusion concept that takes into account countergradient fluxes resulting from large-scale eddies in an unstable, well-mixed atmosphere. The vertical eddy flux within the PBL is given by

$$F_c = -K_c \left(\frac{\partial C}{\partial z} - \gamma_c \right) \tag{12}$$

where γ_c is a "countergradient" transport term describing nonlocal transport due to dry deep convection. The eddy diffusivity is given by the nonlocal formulation

$$K_c = k w_t z \left(1 - \frac{z}{h}^2 \right), \tag{13}$$

where k is the von Karman constant; w_t is a turbulent convective velocity that depends on the friction velocity, height, and the Monin–Obhukov length; and h is the PBL height. The countergradient term for temperature and water vapor is given by

$$\gamma_c = C \frac{{\phi_c}^0}{w_t h}, \tag{14}$$

where C is a constant equal to 8.5, and ${\phi_c}^0$ is the surface temperature or water vapor flux. Equation 14 is applied between the top of the PBL and the top of the surface layer, which is assumed to be equal to $0.1h$. Outside this region and for momentum, γ_c is assumed to be equal to 0.

For the calculation of the eddy diffusivity and countergradient terms, the PBL height is diagnostically computed from

$$h = \frac{\mathrm{Ri_c r}[u(h)^2 + v(h)^2]}{(g/\theta_s)[\theta_v(h) - \theta_s]} \tag{15}$$

where $u(h)$, $v(h)$, and θ_v are the wind components and the virtual potential temperature at the PBL height, g is gravity, $\mathrm{Ri_c r}$ is the critical bulk Richardson number, and θ_s is an appropriate temperature of are near the surface. Refer to (Holtslag et al. 1990) and (Holtslag and Boville 1993) for a more detailed description.

2.2.4 Convective Precipitation Schemes

Convective precipitation is computed using one of three schemes: (1) Grell scheme (Grell 1993); (2) Modified-Kuo scheme (Anthes 1977); and (3) Betts-Miller Scheme. In addition, the Grell parameterization is implemented using one of two closure assumptions: (1) the Arakawa and Schubert closure (Grell et al. 1994a) and (2) the Fritsch and Chappell closure (Fritsch and Chappell 1980), hereafter refered to as AS74 and FC80, respectively.

1. Grell Scheme: The Grell scheme (Grell 1993), similar to the AS74 parameterization, considers clouds as two steady-state circulations: an updraft and a downdraft. No direct mixing occurs between the cloudy air and the environmental air except at the top and bottom of the circulations. The mass flux is constant with height and no entrainment or detrainment occurs along the cloud edges. The originating levels of the updraft and downdraft are given by the levels of maximum and minimum moist static energy, respectively. The Grell scheme is activated when a lifted parcel attains moist convection. Condensation in the updraft is calculated by lifting a saturated parcel. The downdraft mass flux (m_0) depends on the updraft mass flux (m_b) according to the following relation:

$$m_0 = \frac{\beta I_1}{I_2} m_b, \tag{16}$$

where I_1 is the normalized updraft condensation, I_2 is the normalized downdraft evaporation, and β is the fraction of updraft condensation that re-evaporates in the downdraft. β depends on the wind shear and typically varies between 0.3 and 0.5. Rainfall is given by

$$P^{CU} \;=\; I_1 m_b (1-\beta). \tag{17}$$

Heating and moistening in the Grell scheme are determined both by the mass fluxes and the detrainment at the cloud top and bottom. In addition, the cooling effect of moist downdrafts is included.

Due to the simplistic nature of the Grell scheme, several closure assumptions can be adopted. RegCM3's default version directly implements the quasi-equilibrium assumption of AS74. It assumes that convective clouds stabilize the environment as fast as non-convective processes destabilize it as follows:

$$m_b = \frac{ABE'' - ABE}{NA\Delta t}, \tag{18}$$

where ABE is the buoyant energy available for convection, ABE'' is the amount of buoyant energy available for convection in addition to the buoyant energy generated by some of the non-convective processes during the time interval Δt, and NA is the rate of change of ABE per unit m_b. The difference $ABE'' - ABE$ can be thought of as the rate of destabilization over time Δt. ABE'' is computed from the current fields plus the future tendencies resulting from the advection of heat and moisture and the dry adiabatic adjustment.

Another stability based closure assumption that is commonly implemented in GCMs and RCMs is the FC80 type closure assumption. In this closure, it is assumed that convection removes the ABE over a given time scale as follows:

$$m_b = \frac{ABE}{NA\tau}, \tag{19}$$

where τ is the ABE removal time scale.

The fundamental difference between the two assumptions is that the AS74 closure assumption relates the convective fluxes and rainfall to the tendencies in the state of the atmosphere, while the FC80 closure assumption relates the convective fluxes to the degree of instability in the atmosphere. Both schemes achieve a statistical equilibrium

between convection and the large-scale processes. However, this subtle distinction in the implementation of the closure will prove to be an important difference.

2. Kuo Scheme: Convective activity in the Kuo scheme is initiated when the moisture convergence M in a column exceeds a given threshold and the vertical sounding is convectively unstable. A fraction of the moisture convergence β moistens the column and the rest is converted into rainfall P^{CU} according to the following relation:

$$P^{CU} = M(1-\beta). \tag{20}$$

β is a function of the average relative humidity $\overline{RH}$ of the sounding as follows:

$$\beta = \begin{cases} 2(1-\overline{RH}) & \overline{RH} \geq 0.5 \\ 1.0 & \text{otherwise} \end{cases} \tag{21}$$

Note that the moisture convergence term includes only the advective tendencies for water vapor. However, evapotranspiration from the previous time step is indirectly included in M since it tends to moisten the lower atmosphere. Hence, as the evapotranspiration increases, more and more of it is converted into rainfall assuming the column is unstable. The latent heating resulting from condensation is distributed between the cloud top and bottom by a function that allocates the maximum heating to the upper portion of the cloud layer. To eliminate numerical point storms, a horizontal diffusion term and a time release constant are included so that the redistributions of moisture and the latent heat release are not performed instantaneously (Giorgi and Bates 1989),(Giorgi and Marinucci 1991).

3. Betts-Miller Scheme: In the Betts-Miller scheme, the sub-grid scale effects of convective clouds are represented by adjusting temperature and moisture profiles to the observed quasi-equilibrium structures for deep convection and to a mixing line structure for shallow convection. Quasi-equilibrium between the cloud field and the large-scale forcing forms the basis of representing deep convection in the BM scheme. Quasi-equilibrium means that the convective cloud field constrains the thermal and moisture structure of the atmosphere against the destabilizing influence of the large scale flow. The concept has been found to be valid on large spatial and temporal scales. The effects of shallow convection is viewed as a mixing process between the surface layer air and the free atmosphere.

Observational basis for deep convection The thermodynamics of the BM scheme is based on the saturation point formulation as reported in (Betts 1982). The saturation point (sp) is defined as the temperature and pressure (T^*, p^*) at the lifting condensation level (LCL). The subsaturation parameter P is the difference between air parcel saturation level pressure and the actual pressure level i.e. $P = p^* - p$. (Betts 1986) observed that temperature profiles below the freezing level in deep convection is parallel to the θ_{ESV} isopleth, where θ_{ESV} is defined as a constant virtual equivalent potential temperature. This led to the proposal that the reference lapse rate in the lower-troposphere is moist virtual adiabatic rather than the widely accepted moist adiabat. Since the slope of the θ_{ESV} isopleth is 0.9 times that of the moist adiabat, the air parcel buoyancy reduction due to cloud water content is accounted for. This reference structure in the presence of deep convection is universal as reported by (Betts 1986) for the cases of hurricanes,

GATE slow and fast moving squall lines and Venezuela convective episodes. Thus, the reference structure below 600 hPa or the freezing level is the θ_{ESV} with θ_{ES} constrained to a minimum at 600 hPa. Above 600 hPa the observed thermal profile increases to cloud top θ_{ES} value. Considerable variability is associated with the observed moisture structure. Despite this a reference moisture profile is specified in the scheme.

Observational basis for shallow convection: A shallow cumulus cloud field is regarded as a mixing process between the surface layer air and the free atmosphere. This mixing is characterized by a mixing line. Thus when two air parcels mix in the vertical, the *sp* of every possible mixture lies on the mixing line joining the *sp*s of the two parcels. This mixing line structure for shallow cumulus convection was highlighted by (Betts 1982) by plotting *sp*s between 900-700 hPa and the *sp*s were found to lie close to the line joining the *sp*s. This evidence was presented for the undisturbed trade wind region and tropical land stations.

Reference profiles for deep convection: The scheme involves a lagged adjustment of the resolvable-scale T and q_v profile towards a reference quasi-equilibrium structure in the presence of grid-scale radiative and advective processes. The reference T, q_v profiles for deep convection are based on the observation that θ_{ES} (at cloud base) decreases with height upto the freezing level (while being parallel to the θ_{ESV} isopleth) and increasing to θ_{ES} of the environment near the cloud top. The first guess temperature profiles are constructed using

$$\theta_{ES}(p) = \theta_{ES}(B) + \alpha V\,(p - p_B)\,\text{for} p_B > p > p_M \tag{22}$$

where V is the vertical lapse rate of θ_{ESV}, α is the weighting factor set to 1.5 based on the GATE data set and

$$\theta_{ES}(p) = \theta_{ES}(M) + (\theta_{ES}(T) - \theta_{ES}(M))\left(\frac{p - p_T}{p_M - p_T}\right)\text{for} p_T < p < p_M \tag{23}$$

where $\theta_{ES}(T)$ is the environmental saturated equivalent potential temperature at cloud top and $\theta_{ES}(M)$ is the minimum saturated equivalent potential temperature at the freezing level.

The moisture profile is found by specifying the $P = p^* - p$ parameter at three levels (i.e., at the cloud base $P_B = -3875$ Pa, at the freezing level $P_M = -5875$ Pa and at the cloud top $P_T = -1875$ Pa) with linear gradients in between. While the temperature profiles show greater universality, the observed moisture profiles exhibit considerable variability. The above pre-specified profile defined by P_B, P_F and P_T corresponds to a mean profile observed in the tropics. (In the present simulation the average moisture structure is representative of the GATE region squall lines.)

The first guess temperature and moisture profiles are corrected to satisfy the total enthalpy constraint

$$\int_{p_0}^{p_T} \left(k_r - \overline{k}\right) dp = 0 \tag{24}$$

where $k_r = C_p T_R + L q_R$ and T_R, q_R are the first guess reference temperature and specific humidity, respectively. $\overline{k} = C_p \overline{T} + L\overline{q}$, $\overline{T}, \overline{q}$ are the grid mean temperature and specific humidity, before the onset of deep convection.

Reference profiles for shallow convection The first guess profiles for temperature and specific humidity are constructed from properties of the air at the cloud base (pressure

p_B) and air above the cloud top (pressure p_T^+). Equal quantities of air from p_B and p_T^+ are mixed and the corresponding *sp* (i.e., level 1) determined. The slope of the mixing line is found as

$$M = \frac{\theta_E(1) - \theta_E(B)}{P_{SL}(1) - P_{SL}(B)} \tag{25}$$

where B corresponds to the cloud base and P_{SL} is the pressure at saturation levels (i.e., for parcels from cloud base B and the air mixture between p_B and p_T^+). The temperature profile (reference) is parallel to the mixing line and is given by

$$\theta_{ES}(p) = \theta_{ES}(B) + M(p - p_B) \tag{26}$$

$\theta_{ES}(p)$ is inverted to yield T and p, which with the subsaturation parameter (at level 1) gives *sp* and q_v.

The first guess reference T and q_v profiles are corrected to satisfy the following energy constraints:

$$\int_{p_B}^{p_{T+1}} C_p \left(T_R - \overline{T}\right) dp = \int_{p_B}^{p_{T+1}} L \left(q_R - \overline{q}\right) dp = 0 \tag{27}$$

Adjustment time τ: The adjustment time (τ) in the scheme is set such that the atmosphere nearly saturates on the grid scale in the presence of a convective disturbance. According to (Betts and Miller 1993), in the T106 resolution ($\approx 1.125°$) model, τ for deep convection and for shallow convection is 2 h. (Betts 1997) expressed τ as a function of horizontal scales. He found τ to lie between 40-80 min for the T106 resolution model. For $\Delta x = 60$ km, τ lies between 20-40 min. In the present simulation we employ $\tau = 55$ min for deep and shallow convection at $\Delta x = 60$ km resolution.

Downdrafts in the BM scheme

The BM scheme (Betts 1986) was designed primarily for tropical convection. One of the weakness in the original deep convective scheme is the absence of downdrafts. The interaction of deep convection with the ABL processes cannot be captured by the original deep scheme. Furthermore, convective downdraft cooling and drying at low levels can have an impact on convective development downstream through advective effects of the cold and drier air over a period of several hours even under weak surface wind regimes (such as in the WPR where maximum ABL winds are ≤ 7 m s^{-1}). In fact, the motivation to include downdrafts in the original scheme was to mitigate the problem of grid-scale instabilities (Zhang et al. 1988) arising downstream of the island of New Guinea much later in the simulation. The instability arose due to the absence of low-level cold and dry air advection emanating from deep convection present over the island between 0000 - 0600 UTC 15 December 1992.

The original scheme is modified with the inclusion of downdrafts suggested by (Betts and Miller 1993). The downdrafts are parameterized by defining a simple unsaturated downdraft thermodynamic path (constant θ_e and constant subsaturation) originating at 850 hPa level. A different adjustment time for this process is employed and it is a function of evaporation in downdrafts and the deep convective (PR) precipitation. The adjustment time (τ_{ABL}) is given by

$$\frac{1}{\tau_{ABL}} = \frac{\alpha PR}{\int_{p_\circ}^{p_{ABL}} \Delta q_c \frac{dp}{g}} \tag{28}$$

where the constant α is set to -0.10 in this study and is a measure of the precipitation efficiency of the cumulus clouds. dp is the vertical pressure interval, g is the gravitational

acceleration, $p_{\circ} and p_{ABL}$ are the respective pressure at the lowest model level and at the top of the ABL, and Δq_c is the change of q_v along the downdraft descent path. Simply put the temperature and moisture profiles for the downdraft are parallel to the moist adiabat at constant subsaturation. The downdraft air is injected into the 3 lowest model levels (in the ABL).

2.2.5 Large-Scale Precipitation Scheme

Subgrid Explicit Moisture Scheme (SUBEX) is used to handle nonconvective clouds and precipitation resolved by the model. This is one of the new components of the model. SUBEX accounts for the subgrid variability in clouds by linking the average grid cell relative humidity to the cloud fraction and cloud water following the work of (Sundqvist et al. 1989).

The fraction of the grid cell covered by clouds, FC, is determined by,

$$FC = \sqrt{\frac{RH - RH_{min}}{RH_{max} - RH_{min}}} \tag{29}$$

where RH_{min} is the relative humidity threshold at which clouds begin to form, and RH_{max} is the relative humidity where FC reaches unity. FC is assumed to be zero when RH is less than RH_{min} and unity when RH is greater than RH_{max}.

Precipitation P forms when the cloud water content exceeds the autoconversion threshold ${Q^{th}}_c$ according to the following relation:

$$P = C_{ppt}(Q_c/FC - {Q_c}^{th})FC \tag{30}$$

where $1/C_{ppt}$ can be considered the characteristic time for which cloud droplets are converted to raindrops. The threshold is obtained by scaling the median cloud liquid water content equation according to the following:

$${Q^{th}}_c = C_{acs}10^{-0.49+0.013T}, \tag{31}$$

where T is temperature in degrees Celsius, and C_{acs} is the autoconversion scale factor. Precipitation is assumed to fall instantaneously.

SUBEX also includes simple formulations for raindrop accretion and evaporation. The formulation for the accretion of cloud droplets by falling rain droplets is based on the work of (Beheng 1994) and is as follows:

$$P_{acc} = C_{acc}QP_{sum} \tag{32}$$

where P_{acc} is the amount of accreted cloud water, C_{acc} is the accretion rate coefficient, and P_{sum} is the accumulated precipitation from above falling through the cloud.

Precipitation evaporation is based on the work of (Sundqvist et al. 1989) and is as follows,

$$P_{evap} = C_{evap}(1 - RH){P^{1/2}}_{sum} \tag{33}$$

where P_{evap} is the amount of evaporated precipitation, and C_{evap} is the rate coefficient. For a more detailed description of SUBEX and a list of the parameter values refer to (Pal et al. 2000).

2.2.6 Ocean flux Parameterization

1. BATS:
2. Zeng: Sensible heat (SH), latent heat (LH), and momentum (τ) fluxes between the sea surface and lower atmosphere are calculated using the following bulk aerodynamic algorithms,

$$\tau = \rho_a {u_*}^2 ({u_x}^2 + {u_y}^2)^{1/2}/u \tag{34}$$

$$\mathrm{SH} = -\rho_a C_{pa} u_* \theta_* \tag{35}$$

$$\mathrm{LH} = -\rho_a L_e u_* q_* \tag{36}$$

where u_x and u_y are mean wind components, u_* is the frictional wind velocity, θ_* is the temperature scaling parameter, q_* is the specific humidity scaling parameter, ρ_a is air density, C_{pa} is specific heat of air, and L_e is the latent heat of vaporization. For further details on the calculation of these parameters refer to (Zeng et al. 1998).

2.2.7 Pressure Gradient Scheme

Two options are available for calculating the pressure gradient force. The normal way uses the full fields. The other way is the hydrostatic deduction scheme which makes use of a perturbation temperature. In this scheme, extra smoothing on the top is done in order to reduce errors related to the PGF calculation.

2.2.8 Lake Model

The lake model developed by (Hostetler et al. 1993) can be interactively coupled to the atmospheric model. In the lake model, fluxes of heat, moisture, and momentum are calculated based on meteorological inputs and the lake surface temperature and albedo. Heat is transferred vertically between lake model layers by eddy and convective mixing. Ice and snow may cover part or all of the lake surface.

In the lake model, the prognostic equation for temperature is,

$$\frac{\partial T}{\partial t} = (k_e + k_m)\frac{\partial^2 T}{\partial z^2} \tag{37}$$

where T is the temperature of the lake layer, and k_e and k_m are the eddy and molecular diffusivities, respectively. The parameterization of (Henderson-Sellers 1986) is used to calculate k_e and k_m is set to a constant value of $39 \times 10^{-7}\ m^2\ s^{-1}$ except under ice and at the deepest points in the lake.

Sensible and latent heat fluxes from the lake are calculated using the BATS parameterizations (Dickinson et al. 1993). The bulk aerodynamic formulations for latent heat flux (F_q) and sensible heat flux (F_s) are as follows,

$$F_q = \rho_a C_D V_a (q_s - q_a) \tag{38}$$

$$F_s = \rho_a C_p C_D V_a (T_s - T_a) \tag{39}$$

where the subscripts s and a refer to surface and air, respectively; ρ_a is the density of air, V_a is the wind speed, C_p, q is specific humidity, and T is temperature. The momentum drag coefficient, C_D, depends on roughness length and the surface bulk Richardson number. Under ice-free conditions, the lake surface albedo is calculated as a function of solar zenith angle (Henderson-Sellers 1986). Longwave radiation emitted from the lake is calculated according to the Stefan-Boltzmann law. The lake model uses the partial ice cover scheme of (Patterson and Hamblin 1988) to represent the different heat and moisture exchanges between open water and ice surfaces and the atmosphere, and to calculate the surface energy of lake ice and overlying snow. For further details refer to (Hostetler et al. 1993) and (Small and Sloan 1999).

2.2.9 Tracer Model

"Tracer" is a generic term used to design quantities other than classical meteorological variables transported by and interacting with the physics of RegCM. Due to their climatic impact, aerosols and gases are the first tracers of interest that we consider here. For these quantities, the model solves a prognostic equation of the form (Qian et al. 2001),

$$\frac{\partial \chi}{\partial t} = -\overline{V} \cdot \nabla \chi + F_H + F_V + T_{CUM} + S_\chi - R_{w,ls} - R_{w,cum} - D_{dep} + \sum Q_p - Q_l \quad (40)$$

where the first term on the right hand side represents the horizontal and vertical advection, which are solved using a relaxed upstream scheme; F_H and F_V are horizontal and vertical turbulent diffusion treated in a same way as for water vapor; T_{CUM} is the subgrid transport linked to convection (using well-mixing approximation (Qian et al. 1999) or mass flux transport); S is the source term prescribed from external data, R_w, ls and $R_{w,cum}$ are wet removal by large scale and cumulus clouds (Giorgi 1989); D_{dep} is the dry deposition on surface (depending on the tracer nature, its concentration at lower levels and surface type), Q_p and Q_l represent the production and loss terms, respectively, linked to physico-chemical transformations (depending on the nature of tracer, for example, the chemistry of sulfate aerosol (Qian et al. 2001).

The prognostic concentrations, together with specific optical properties of aerosols are then used to calculate the atmospheric column optical properties required by the radiation scheme and ensuing climatic impact (Giorgi et al. 2002). A parameterization of the aerosol indirect effect (modification of cloud properties) has also been introduced (e.g. (Qian et al. 1999)).

3 Pre-Processing

Before performing a regional climate simulation there are two pre-processing steps that need to be completed. The first step involves defining the domain and grid interval, and interpolating the landuse and elevation data to the model grid. This task is performed in the **RegCM/PreProc/Terrain** sub-directory. The second step is to generate the files used for the initial and boundary conditions during the simulation. This step is performed in the **RegCM/PreProc/ICBC** sub-directory. All of input data necessary to run the model can be downloaded from the PWC website at the following URL:

http://www.ictp.trieste.it/~pubregcm/RegCM3

Input data used by the **Terrain** and **ICBC** programs are stored in the **RegCM/PreProc/DATA** sub-directory. A script called *datalinker.x* is provided in this directory in case the data exists elsewhere. It can be modified and run to create soft links between the **RegCM/PreProc/DATA** sub-directory and some other directory.

The present version of RegCM3 support multi-planform of UNIX (or LINUX) operation system, such as IBM, SGI, SUN, DEC, and PC-LINUX (with PGI FORTRAN compiler or Intel IFC FORTRAN compiler). You must make your choices of Makefile under PreProc/Terrain, PreProc/ICBC, and Main/ directories by copying the appropriate Makefile.

Table 1: Land Cover/Vegetation classes

1.	Crop/mixed farming
2.	Short grass
3.	Evergreen needleleaf tree
4.	Deciduous needleleaf tree
5.	Deciduous broadleaf tree
6.	Evergreen broadleaf tree
7.	Tall grass
8.	Desert
9.	Tundra
10.	Irrigated Crop
11.	Semi-desert
12.	Ice cap/glacier
13.	Bog or marsh
14.	Inland water
15.	Ocean
16.	Evergreen shrub
17.	Deciduous shrub
18.	Mixed Woodland
19.	Forest/Field mosaic
20.	Water and Land mixture

3.1 Terrain

Table 2: BATS vegetation/land-cover

Parameter	Land Cover/Vegetation Type																			
	1	2	3	4	5	6	7	8	9	10	11	12	13	14	15	16	17	18	19	20
Max fractional vegetation cover	0.85	0.80	0.80	0.80	0.80	0.90	0.80	0.00	0.60	0.80	0.35	0.00	0.80	0.00	0.00	0.80	0.80	0.80	0.80	0.80
Difference between max fractional vegetation cover and cover at 269 K	0.6	0.1	0.1	0.3	0.5	0.3	0.0	0.2	0.6	0.1	0.0	0.4	0.0	0.0	0.2	0.3	0.2	0.4	0.4	
Roughness length (m)	0.08	0.05	1.00	1.00	0.80	2.00	0.10	0.05	0.04	0.06	0.10	0.01	0.03	0.0004	0.0004	0.10	0.10	0.80	0.3	0.3
Displacement height (m)	0.0	0.0	9.0	9.0	0.0	18.0	0.0	0.0	0.0	0.0	0.0	0.0	0.0	0.0	0.0	0.0	0.0	0.0	0.0	0.0
Min stomatal resistence (s/m)	45	60	80	80	120	60	60	200	80	45	150	200	45	200	200	80	120	100	120	120
Max Leaf Area Index	6	2	6	6	6	6	6	0	6	6	6	0	6	0	0	6	6	6	6	6
Min Leaf Area Index	0.5	0.5	5	1	1	5	0.5	0	0.5	0.5	0.5	0	0.5	0	0	5	1	3	0.5	0.5
Stem (& dead matter) area index)	0.5	4.0	2.0	2.0	2.0	2.0	2.0	0.5	0.5	2.0	2.0	2.0	2.0	2.0	2.0	2.0	2.0	2.0	2.0	2.0
Inverse square root of leaf dimension ($m^{-1/2}$)	10	5	5	5	5	5	5	5	5	5	5	5	5	5	5	5	5	5	5	5
Light sensitivity factor (m^2 W^{-1})	0.02	0.02	0.06	0.06	0.06	0.06	0.02	0.02	0.02	0.02	0.02	0.02	0.02	0.02	0.02	0.02	0.02	0.06	0.02	0.02
Upper soil layer depth (mm)	100	100	100	100	100	100	100	100	100	100	100	100	100	100	100	100	100	100	100	100
Root zone soil layer depth (mm)	1000	1000	1500	1500	2000	1500	1000	1000	1000	1000	1000	1000	1000	1000	1000	1000	1000	2000	2000	2000
Depth of total soil (mm)	3000	3000	3000	3000	3000	3000	3000	3000	3000	3000	3000	3000	3000	3000	3000	3000	3000	3000	3000	3000
Soil texture type	6	6	6	6	7	8	6	3	6	6	5	12	6	6	6	6	5	6	6	0
Soil color type	5	3	4	4	4	4	4	1	3	3	2	1	5	5	5	4	3	4	4	0
Vegetation albedo for wavelengths < 0.7 μ m	0.10	0.10	0.05	0.05	0.08	0.04	0.08	0.20	0.10	0.08	0.17	0.80	0.06	0.07	0.07	0.05	0.08	0.06	0.06	0.06
Vegetation albedo for wavelengths > 0.7 μ m	0.30	0.30	0.23	0.23	0.28	0.20	0.30	0.40	0.30	0.28	0.34	0.60	0.18	0.20	0.20	0.23	0.28	0.24	0.18	0.18

The Terrain program horizontally interpolates the landuse and elevation data from a latitude-longitude grid to the cartesian grid of the chosen domain. RegCM currently uses the Global Land Cover Characterization (GLCC) datasets for the vegetation/landuse data. The GLCC dataset is derived from 1 km Advanced Very High Resolution Radiometer (AVHRR) data spanning April 1992 through March 1993, and is based on the vegetation/land cover types defined by BATS (Biosphere Atmosphere Transfer Scheme). The 18 vegetation/land cover types and associated parameters are presented in Table 2. Each grid cell of the model is assigned one of the eighteen categories. More information regarding GLCC datasets can be found at **http://edcdaac.usgs.gov/glcc/glcc.html**.

The elevation data used is from the United States Geological Survey (USGS). Both the landuse and elevation data files are available at 30 and 10 minute resolutions and can be downloaded from the ICTP PWC website at the following URL,

http://www.ictp.trieste.it/∼pubregcm/RegCM3/DATA/SURFACE

Parameters such as domain size, input data, and length of simulation are defined in the **RegCM/PreProc/Terrain/***domain.param* file (Table 3). After editing this file, running the *terrain.x* script will compile and execute the terrain program. This will generate the output file *DOMAIN.INFO* containing elevation, landuse type, and other variables (Table 4) in the **RegCM/Input** sub-directory. A GrADS descriptor file, *DOMAIN.CTL* is also created.

3.2 ICBC

The ICBC program interpolates sea surface temperature (SST) and global re-analysis data to the model grid. These files are used for the initial and boundary conditions during the simulation. (Eventually, interfaces will exist to allow GCM output to be used for initial and boundary conditions.)

3.2.1 Sea surface temperature

In the **RegCM/PreProc/Terrain/***domain.param* file, there are two options for SST data. One is the Global Sea Surface Temperature (GISST) one-degree monthly gridded data (1871-2002) available from the Hadley Centre Met Office **(http://badc.nerc.ac.uk/data/gisst/)** (note: special permission is needed from the Hadley Center Met Office to use the GISST datasets). Also available is the Optimum Interpolation Sea Surface Temperature (OISST) one-degree weekly analysis (1981-2002) available from the National Ocean and Atmosphere Administration **(http://www.cdc.noaa.gov/)**.

3.2.2 Initial and Boundary Conditions

In the **RegCM/PreProc/Terrain/***domain.param* file, there are three options to choose from for the global analysis datasets to use for the initial and boundary conditions.

• **ECMWF**: The European Centre for Medium-Range Weather Forecasts Reanalysis datasets (T42,L15) from 1993–1997.

• **NNRP1**: The National Center for Environmental Prediction (NCEP) Reanalysis datasets (2.5 degree grid, L17) from 1948–2001.

• **NNRP2**: The National Center for Environmental Prediction (NCEP) Reanalysis datasets (2.5 degree grid, L17) from 1979–2001.

The numerical treatment of the lateral boundaries is a difficult but very important aspect of the regional climate model. There are five types of boundary conditions that can be used in the model.

• **Fixed**: This will not allow time variation at lateral boundaries. Not recommended for real-data applications.

• **Time-dependent**: Outer two rows and columns have specified values of all predicted fields. Recommended for nests where time-dependent values are supplied by the parent domain. Not recommended for coarse mesh where only one outer row and column would be specified.

• **Linear relaxation**: Outer row and column is specified by time-dependent value, next four points are relaxed towards the boundary values with a relaxation constant that decreases linearly away from the boundary.

• **Sponge**: (Perkey and Kreitzberg 1976)

• **Exponential relaxation**: (Davies and Turner 1977) (default)

Note: The type of boundary conditions used in the simulation is selected in the **RegCM/PreProc/Terrain/***domain.param* file.

It is not necessary to modify any files in the **RegCM/PreProc/ICBC** sub-directory. The *SST_1DEG.f* and *ICBC.f* programs interpolate the SST and global analysis data to the model grid. Running the *icbc.x* script will compile and execute these programs. The following files will be generated;

RegCM/Input/ICBC.YYYYMMDDHH (see Table 11 for list of variables)
RegCM/Input/ICBC.YYYYMMDDHH.CTL

4 RegCM

All of the source code for the model is in the **RegCM/Main** sub-directory. The **RegCM/Commons** sub-directory contains two files necessary for running a new simulation. Physics options discussed in Section 2.2 are selected in the *regcm.in* file (Table 7). Restart, timestep, and output frequency parameters are also defined in *regcm.in* (Table 13). The *regcm.x* script will compile and execute the model. It is recommended to create a new directory for specific projects and to copy these files into this new project directory. Running the script will,

- Create soft links to the domain file and initial and boundary conditions files.

  fort.10 → **../Input/***DOMAIN*
  fort.7x → **../Input/***ICBCYYYYMMDDHH*

- Create the sub-directory **output** where the model output files are written.

- Create the *postproc.in* file which will be needed for postprocessing the output files. (This is discussed in the next section.)

- Compile the source code and run the simulation.

Running the model generates the following output files,

Atmospheric model output (see Table 8)

ATM.YYYYMMDDHH

Land surface model output (see Table 9)

SRF.YYYYMMDDHH

Radiation model output (see Table 10)
RAD.YYYYMMDDHH

and a file used to restart the simulation,

SAVTMP.YYYYMMDDHH

5 Post-processing

The postprocessor takes the model output files and generates new output files of averaged variables in commonly used formats such as NetCDF or GrADS. You can modify the *postproc.in* file to specify which of the following files to generate.

- Atmospheric Output (see Table 8 for list of variables)

ATMYYMM.NC	(all atmos variables and times)
ATMYYMMAVG.NC	(all variables atmos averaged)
ATMYYMMDIUR.NC	(diurnal cycle averages of atmos variables)
ATMYYMMCONT.NC	(continual averages of atmos variables)

- Land Surface Model Output (see Table 9 for list of variables)

SRFYYMM.NC	(all surface model variables and times)
SRFYYMMAVG.NC	(all variables surface model averaged)
SRFYYMMDIUR.NC	(diurnal cycle averages of surface model variables)
SRFYYMMCONT.NC	(continual averages of surface model variables)

- Radiation Model Output (Table 10 for list of variables)

RADYYMM.NC	(all radiation variables and times)
RADYYMMAVG.NC	(all variables radiation averaged)
RADYYMMDIUR.NC	(diurnal cycle averages of radiation variables)
RADYYMMCONT.NC	(continual averages of radiation variables)

6 Practice Run

The purpose of this section is to help new users become familiar with setting up and running RegCM by going through a practice run. A step-by-step tutorial is presented for performing one-month simulation over a south Asian domain for July 1991. To demonstrate how to use restart option, first a 5 day simulation is run in June, then the model is restarted and run for an additional 31 days in July.

In this practice run, the 10 minute resolution GLCC and GTOPO datasets are used to create the terrain file, and ECMWF global reanalysis datasets are used for the initial and boundary conditions. You will create links from your working directory to the directories where these data are using the **RegCM/PreProc/DATA/***datalinker.x* script.

6.1 Getting the model code and data

STEP 1. Create a working directory for yourself.

→ mkdir *yourname*
→ cd *yourname*

STEP 2. Download *regcm.tar.gz* to your account from the RegCM3 website at, **http://www.ictp.trieste.it/∼pubregcm/RegCM3/**.

STEP 3. Uncompress and untar *regcm.tar.gz*

→ gzip d *regcm.tar.gz*
→ tar xvf *regcm.tar*

Untarring *regcm.tar.gz* will create a main directory called **RegCM** and several subdirectories containing all the files needed for pre-processing, running the model, and post-processing. Preprocessing programs are in the The **RegCM/PreProc/Terrain** and **RegCM/PreProc/ICBC** sub-directories, the model source code is in the **RegCM/Main** sub-directory, and the postprocessing programs are in the **RegCM/PostProc** and // **RegCM/PostProc-v5d** sub-directories.

6.2 Pre-processing

Several pre-processing steps are necessary before running a simulation. These steps involve setting up the model domain and creating the necessary initial and boundary conditions files.

6.2.1 Setting up the domain

The first step is to define the domain and interpolate elevation and land-use data to the grid. This is done in the **RegCM/PreProc/Terrain** sub-directory. For this practice run we use a south Asian domain of 6300 km × 7440 km size centered over India (21.0° N, 78.0° E) and a horizontal grid-point spacing of 60 km. The domain parameters are defined in the *domain.param* file and the values used for practice run are listed in Table 12.

STEP 1. Link the necessary data files to the **RegCM/PreProc/DATA** sub-directory.

go into the DATA subdirectory,
→ cd RegCM/PreProc/DATA

edit the datalinker script using a text editor such as xemacs,
→ xemacs *datalinker.x*

execute the datalinker script,
→ ./datalinker.x

STEP 2. Go into the Terrain sub-directory and edit the *domain.param* file which contains information regarding domain and grid parameters.

go into the TERRAIN subdirectory,
→ cd RegCM/PreProc/Terrain

edit the domain.param file,
→ xemacs *domain.param*

STEP 3. Run the *terrain.x* script. This compiles code and creates an executable file called *terrain* that is used to generate the *DOMAIN* file, and creates two symbolic links, *CAT.CDF* and *ELEV.CDF*, to the landuse and elevation datasets, respectively.

copy the appropriate Makefile according to what kind of machine your working on,
→ cp Makefile_PGI Makefile
execute the terrain script,
→ *./terrain.x*

This will generate two files in the **RegCM/Input** sub-directory, *DOMAIN.INFO* and *DOMAIN.CTL* (See Table 4 for a list of variables).

To view the file in GrADS,

go into the Input subdirectory,
→ cd **RegCM/Input**

open GrADS,
→ '**grads**' (opens GrADS)

grads → open *DOMAIN.CTL* (opens file in GrADS)
grads → q file (list variables in *DOMAIN*)
grads → d ht (displays elevation contours over domain)

6.2.2 ICBC

The second step is to interpolate the sea surface temperature and global analysis data that will be used for the initial and boundary conditions to the model grid. This step is performed in the **RegCM3/PreProc/ICBC** sub-directory.

STEP 1. Go into the ICBC sub-directory and execute the icbc script. It is not necessary to modify any files in this directory. Simply run the *icbc.x* script and it will create and run the executables to generate the files for initial and boundary conditions.

copy the appropriate Makefile according to what kind of machine your working on,
→ cp Makefile_PGI Makefile

→ cd **RegCM/PreProc/ICBC**
→ *./icbc.x*

This will generate two files in the **RegCM/Input** sub-directory, *ICBC1991062500* and *ICBC1994062500.CTL*. These files are used to for the initial and boundary conditions during the simulation.

6.3 Running the Model

It is convenient to create a new directory for your simulation where the executable file and model output files will be written.

STEP 1. Create a sub-directory called **RegCM/PracticeRun** and copy the *regcm.in* and *regcm.x* in the **RegCM/Commons** subdirectory to it.

make a second level subdirectory called PracticeRun,
→ mkdir **PracticeRun**

go into the new subdirectory PracticeRun,
→ cd **PracticeRun**

copy the two files, regcm.in and regcm.x, from the Commons subdirectory,
→ cp **../Commons/***regcm.in* .
→ cp **../Commons/***regcm.x* .

STEP 2. Before running the simulation you only need to modify the the *regcm.in* file. This file contains parameters regarding the use of restart files and physics options. Edit the file according to the parameters defined in Table 13 and Table 14. First, a 5-day simulation from 25 June 1991 00 UTC through 30 June 1991 00 UTC will be performed.

edit the regcm.in file,
→ xemacs *regcm.in*

copy the appropriate Makefile in the Main subdirectory according to what kind of ma-

chine you are working on,
→ cp ../Main/Makefile_PGI ../Main/Makefile

STEP 3. Run the *regcm.x* script. This will compile the source code and start the simulation.

→ *./regcm.x*

After the simulation is completed you will have the following monthly files of model output in the **RegCM/PracticeRun/output** sub-directory,

ATM.1991062500 - output from the atmospheric model
RAD.1991062500 - output from the radiation model
SFC.1991062500 - output from the land surface model
SAV.1991062500 - restart file

6.3.1 Restarting the model

To restart the model you only need to modify a few parameters in the *regcm.in* file.
STEP 1. Edit the the following restart parameters in the *regcm.in* file.

- ifrest = .true. (indicates this is a restart simulations)
- idate0 = 1994070100 (start date of first simulation)
- idate1 = 1994070600 (start date for restart simulation)
- idate2 = 1994080100 (end date for restart simulation)

STEP 3. Run the *regcm.x* script to restart the simulation.

→ *./regcm.x*

After the simulation is complete you will have the following monthly files of model output in the **RegCM/PracticeRun/output** sub-directory,

ATM.1991070100 - output from the atmospheric model
RAD.1991070100 - output from the radiation model
SFC.1991070100 - output from the land surface model
SAV.1991070100 - restart file

Table 3: List of variables defined in *domain.param* file.

Parameter	Description
iy	number of grid points in y direction (i)
jx	number of grid points in x direction (j)
kz	number of vertical levels (k)
ds	grid point separation in km
ptop	pressure of model top in cb
clat	central latitude of model domain in degrees
clon	central longitude of model domain in degrees
plat	pole latitude (only for rotated mercator projection)
plon	pole longitude (only for rotated mercator projection)
ntypec	resolution of the global terrain and land-use data 1 = 1 degree 144 = 5 minute 4 = 30 minute 400 = 3 minute 36 = 10 minute 900 = 2 minute
nveg	vegetation dataset 13 = MM4 Vegetation 20 = GLCC Vegetation (must set ntypec=36)
iproj	map projection 'LAMCON' = Lambert Conformal 'POLSTR' = Polar Stereographic 'NORMER' = Normal Mercator 'ROTMER' = Rotated Mercator
h2ofrac	if water fraction < h2ofrac, then land else water
ifanal	true=perform cressman-type objective analysis false=perform 16-point overlapping parabolic interpolation
smthbdy	true=extra smoothing in boundaries
prtflds	true=print fields to display (eg. heights, landuse)
lakadj	true=adjust lake levels according to obs
filout	terrain output filename including path
filctl	GrADS control filename for output including path
IDATE1	beginning date of simulation (YYYYMMDDHH)
IDATE2	ending date of simulation (YYYYMMDDHH)
SSTTYP	SST dataset 'OISST' 'OI_NC' 'GISST' 'OI_WK' for FVGCM; 'RF' 'A2' 'B2'
DATTYP	global analysis dataset 'ECMWF' 'FVGCM' 'NNRP1' 'FNEST' 'NNRP2'
igrads	true=output GrADS control file
ibigend	0 = little-endian binary computer (PC LINUX, DEC) 1 = big-endian binary computer (SUN, SGI, IBM, PC LINUX with PGI or IFC)
IOMEGA	use vertical winds in boundary conditions
FUDGE	land-sea mask fudge, true or false

Table 4: List of output variables from Terrain (DOMAIN)

Variables	**Description**
ht	Surface elevation (m)
htsd	Surface elevation standard deviation
landuse	Surface landuse type
xlat	Latitude of cross points
xlon	Longitude of cross points
dlat	Latitude of dot points
dlon	Longitude of dot points
xmap	Map factors of cross points
dmap	Map factors of dot points
coriol	Coriolis force
snowam	Initial snow amount

Table 5: List of variables in *ICBCYYYYMMDDHH* files

Variables	**Description**
u	Westerly wind (m s^{-1})
v	Southerly wind (m s^{-1})
t	Air temperature (K)
q	Specific moisture (kg kg^{-1})
px	Surface pressure (hPa)
ts	Surface air temperature (K)

Table 6: List of restart, timestep, and output parameters defined in *regcm.in* file.

Restart parameters	**Description**
ifrest	true or false for restart simulation
idate0	start date of first simulation
idate1	restart date
idate2	end date of restart simulation
nslice	number of days for next model run
Timestep parameters	**Description**
radfrq	time step for radiation model
abemh	time step for LW absorption/emissivity
abatm	time step for lsm
dt	time step for atmosphere model
ibdyfrq	lateral boundary conditions frequency
Output parameters	**Description**
ifsave	save output for restart
savfrq	time interval to save output for restart (hr)
iftape	save atmospheric output
tapfrq	time interval to save atmospheric output (hr)
ifrad	save radiation output
radisp	time interval to save radiation output (hrs)
ifbat	save surface model output
batfrq	time interval to save surface model output (hrs)
ifprt	printer output
prtfrq	time interval for printer output (hrs)
kxout	k level of horizontal slice for printer output
jxsex	j index of the north-south vertical slice for printer output
iotyp	Output format; 1=direct access, 2=sequential
ibintyp	1=big_endian, 2=little_endian
ifchem	save tracer model output
chemfrq	time interval to save tracer model output (hrs)

Table 7: List of physic options in *regcm.in* file.

Physics parameter	**Description**
iboudy	lateral boundary conditions; 0=fixed, 1=relaxation (linear), 2=time dependent, 3=time and inflow/outflow dependent 4=sponge, 5=relaxation (exponential)
ibltyp	planetary boundary layer scheme; 1=Holtslag
icup	cumulus scheme; 1=Anthes-Kuo, 2=Grell, 3=Betts-Miller
igcc	Grell Scheme Convective Closure Scheme; 1=Arakawa & Schubert, 2=Fritsch & Chappell
ipptls	Large-scale precipitation scheme; 1=SUBEX
iocnflx	ocean flux parameterization scheme; 1= BATS, 2=Zeng
ipgf	pressure gradient scheme; 0=normal way, 1= hydrostatic deduction
lakemod	Lake model; 0=no, 1=yes
ichem	Tracer/Chemistry model; 0=no, 1=yes
SUBEX parameter	**Description**
ncld	number of bottom model levels without clouds
fcmax	maximum cloud cover fraction
qck1land/qck1oce	autoconversion rate for land/ocean
gulland/guloce	fraction of Gultepe eqn (qcth) when precip occurs over land/ocean
rhmax	RH at which FCC = 1.0
rh0oce/rh0land	RH threshold for ocean/land
cevap	raindrop evap rate coef [[(kg m^{-2} s^{-1})$^{-1/2}$]]
caccr	raindrop accretion rate (m^3 kg^{-1} s^{-1})
Grell parameter	**Description**
shrmin/shrmax	minimum/maximum shear effect on precip eff.
edtmin/edtmax	minimum/maximum precip efficiency
edtmino/edtmaxo	minimum/maximum precip efficiency (o var)
edtminx/edtmaxx	minimum/maximum precip efficiency (x var)
pbcmax	max depth (mb) of stable layer between LCL & LFC
mincld	minimum cloud depth (mb)
htmin/htmax	minimum/maximum convective heating
skbmax	maximum cloud base height in sigma coords.
dtauc	Fritsch & Chappell (1980) ABE Removal Timescale (min)
Chemistry parameters	**Description**
ichremlsc	aerosol wet removal from large-scale clouds
ichremcvc	aerosol wet removal from convective clouds
ichdrdepo	aerosol dry deposition on surface
ichcumtra	convective transport of aerosols
idirect	direct radiative effect of aerosols

Table 8: List of output variables from atmosphere

Variables	Description
u	Zonal wind (m s^{-1})
v	Meridional wind (m s^{-1})
tk	Temperature (K)
qd	Mixing ratio (g kg^{-1})
qc	Cloud mixing ratio (g kg^{-1})
ps	Surface pressure (Pa)
rt	Total precipitation (mm)
tgrnd	Geopotential height (gpm)
smt	Total soil water (mm)
rb	Base flow (mm day^{-1})

Table 9: List of output variables from surface model

Variables	Description
ua	Anemometer zonal winds (m s^{-1})
va	Anemometer meridional winds (m s^{-1})
drag	Surface drag stress
tg	Ground temperature (K)
tf	Foliage temperature (K)
ta	Anemometer temperature (K)
qa	Anemometer specific humidity kg kg^{-1}
smu	Top layer soil moisture (mm)
smr	Root layer soil moisture (mm)
rt	Total precipitation (mm day^{-1})
et	Evapotranspiration (mm day^{-1})
rnfs	Surface runoff (mm day^{-1})
snow	Snow water equivalent (mm)
sh	Sensible heat (W m^{-2})
lwn	Net longwave (W m^{-2})
swn	Net solar absorbed (W m^{-2})
lwd	Downward longwave (W m^{-2})
swi	Solar incident (W m^{-2})
rc	Convective precipitation (mm day^{-1})
psrf	Surface pressure (Pa)
zpbl	PBL height (m)

Table 10: List of output variables from radiation model

Variables	Description
fc	Cloud fraction (fraction)
clwp	Cld liquid H_2O path (g m^{-2})
qrs	Solar heating rate (K s^{-1})
qrl	LW cooling rate (K s^{-1})
fsw	Surface abs solar (W m^{-2})
flw	LW cooling of surface (W m^{-2})
clrst	Clear sky col abs sol (W m^{-2})
clrss	Clear sky surf abs sol (W m^{-2})
clrlt	Clear sky net up flux (W m^{-2})
clrls	Clear sky LW surf cool (W m^{-2})
solin	Instant incid solar (W m^{-2})
sabtp	Column abs solar (W m^{-2})
firtp	Net up flux at top (W m^{-2})

Table 11: List of output variables from tracer model

Variables	Description
trac	Tracer mixing ratio (kg kg^{-1})
col_tr	Column burden (kg m^{-2})
wdlsc_tr	Wet deposition large-scale (kg m^{-2})
wdcvc_tr	Wet deposition convective (kg m^{-2})
sdrdp_tr	Wet deposition large-scale (kg m^{-2})
emiss_tr	Surface dry deposition (kg m^{-2})

Table 12: List of variables to be modified in *domain.param* file.

Parameter	Value	Description
iy	105	number of grid points in y direction (i)
jx	124	number of grid points in x direction (j)
kz	18	number of vertical levels (k)
ds	60.0	grid point separation in km
ptop	7.0	pressure of model top in cb
clat	21.0	central latitude of model domain in degrees
clon	78.0	central longitude of model domain in degrees
ntypec	36	resolution of the global terrain and land-use data
nveg	20	vegetation dataset
iproj	'ROTMER'	map projection
igrads	1	true=output GrADS control file
IDATE1	1994070100	beginning date of simulation
IDATE2	1994080100	ending date of simulation
SSTTYP	'OISST'	SST dataset
DATTYP	'ECMWF'	global analysis dataset

Table 13: List of variables to be modified in *regcm.in* file.

Parameter	Value	Description
ifrest	.false.	restart file
idate0	1991062500	restart file
idate1	1991072500	restart file
idate2	1991063000	restart file
savfrq	24.	time interval to save output (hrs) for restart
iftape	.true.	save atmospheric output
tapfrq	6.	time interval to save atmospheric output
ifrad	.true.	save radiation output
radisp	6.	time interval to save radiation output (hrs)
ifbat	.true.	save surface model output
batfrq	3.	time interval to save surface model output (hrs)
ifprt	.false.	printer output

Table 14: List of variables to be modified in *regcm.in* file.

Parameter	Value	Description
iboudy	5	lateral boundary conditions; 0=fixed, 1=relaxation (linear), 2=time dependent, 3=time and inflow/outflow dependent 4=sponge, 5=relaxation (exponential)
ibltyp	1	planetary boundary layer scheme; 1=Holtslag
icup	2	cumulus parameterization scheme; 1=Anthes-Kuo, 2=Grell, 3=Betts-Miller
igcc	2	Grell Scheme Convective Closure Scheme; 1=Arakawa & Schubert, 2=Fritsch & Chappell
ipptls	1	Large-scale precipitation scheme; 1=SUBEX
iocnflx	2	ocean flux parameterization scheme; 1= BATS, 2=Zeng
ipgf	0	pressure gradient scheme; 0=normal way, 1= hydrostatic deduction
lakemod	0	Lake model; 0=no, 1=yes
radfrq	30.	time freq for solar rad calculation (min)
abemh	18.	time freq for surface model (min)
abatm	600.	time freq for absorption/emission calculation (min)
dt	200.	time step in seconds
ibdyfrq		boundary condition interval (hours)
ncld	3	# of bottom model levels without clouds
fcmax	0.80	maximum cloud cover fraction
qck1land	5.e-4	autoconversion rate for land
qck1oce	5.e-4	autoconversion rate for ocean
gulland	0.4	fraction of Gultepe eqn (qcth) when precip occurs (land)
guloce	0.4	fraction of Gultepe eqn (qcth) when precip occurs (ocean)
rhmax	1.01	RH at which FCC = 1.0
rh0oce	0.90	RH threshold for ocean
rh0land	0.80	RH threshold for land
cevap	1.e-5	raindrop evap rate coef [[(kg m^{-2} s^{-1})$^{-1/2}$]]
caccr	6.0	raindrop accretion rate (m^3 kg^{-1} s^{-1})
shrmin	0.25	minimum shear effect on precip eff.
shrmax	0.50	maximum shear effect on precip eff.
edtmin	0.25	minimum precip efficiency
edtmax	1.0	maximum precip efficiency
edtmino	0.0	minimum precip efficiency (o var)
edtmaxo	1.0	maximum precip efficiency (o var)
edtminx	0.25	minimum precip efficiency (x var)
edtmaxx	1.0	maximum precip efficiency (x var)
pbcmax	150.0	max depth (mb) of stable layer between LCL & LFC
mincld	150.0	minimum cloud depth (mb)
htmin	-250.0	minimum convective heating
htmax	500.0	maximum convective heating
skbmax	0.4	maximum cloud base height in sigma coords.
dtauc	30.0	Fritsch & Chappell (1980) ABE Removal Timescale (min)

References

Anthes, R. (1977). A cumulus parameterization scheme utilizing a one-dimensional cloud model, *Monthly Weather Review* .

Anthes, R. A., Kuo, Y.-H., Low-Nam, S., Hsie, E.-Y. and Bettge, T. M. (1989). Estimation of episodic and climatological skill and uncertainty in regional numerical models, *Quarterly Journal of the Royal Meteorological Society* .

Anthes, R., Hsie, E. and Kuo, Y.-H. (1987). Description of the penn state / ncar mesoscale model version 4 (mm4), ncar tech. note. ncar/tn-282, *Technical report*, National Center for Atmospheric Research.

Anthes, R., Seaman, N. and Warner, T. (1980). Comparisons of numerical simulations of the planetary boundary layer by a mixed-layer and multi-level model, *Monthly Weather Review* .

Anthes, R. T. W. (1978). Development of hydrodynamic models suitable for air pollution and other mesometeorological studies, *Monthly Weather Review* .

Bates, G., Giorgi, F. and Hostetler, S. (1993). Towards the simulation of the effects of the great lakes on regional climate, *Monthly Weather Review* .

Bates, G., Hostetler, S. and Giorgi, F. (1995). Two-year simulation of the great lakes region with a coupled modeling system, *Monthly Weather Review* .

Bates, G. T. (1990). A case study of the effects of topography on cyclone development in the western united states, *Monthly Weather Review* .

Beheng, K. (1994). A parameterization of warm cloud microphysical conversion processes, *Atmospheric Research* .

Betts, A. (1982). Cloud thermodynamic models in saturation point coordinates, **39**: 2182–2191.

Betts, A. (1986). A new convective adjustment scheme. Part I: Observational and theoretical basis, **112**: 667–691.

Betts, A. (1997). The parameterization of deep convection, *in* R. Smith (ed.), *The physics and parameterization of moist atmospheric convection*, Kluwer Academic Publishers, pp. 255–279.

Betts, A. and Harshavardhan (1987). Thermodynamic constraint on the cloud liquid water feedback in climate models, **92**: 8483–8485.

Betts, A. K. and Miller, M. (1993). The Betts-Miller scheme, Chapter 9, *The representation of cumulus convection in numerical models of the atmosphere*, (Eds. K.A. Emanuel and D.J. Raymond),Meteo. Mon., American Meteorological Society, pp. 107–121.

Blackadar, A. (1979). Boundary layer wind maxima and their significance for the growth of nocturnal inversions, *Bulletin of the American Meteorological Society* .

Briegleb, B. (1992). Delta-eddington approximation for solar radiation in the ncar community climate model, *Journal of Geophysical Research* .

Climate Processes and Climate Sensitivity (1984). American Geophysical Union, chapter Modeling evapotranspiration processes for three-dimensional global climate models.

Dai, A., Giorgi, F. and Trenberth, K. E. (1999). Observed and model-simulated diurnal cycles of precipitation over the contiguous united states, *Journal of Geophysical Research* .

Davies, H. and Turner, R. (1977). Updating prediction models by dynamical relaxation: An examination of the technique, *Quarterly Journal of the Royal Meteorological Society* .

Deardoff, J. (1978). Efficient prediction of ground surface temperature and moisture with inclusion of a layer of vegetation, *Journal of Geophysical Research* .

Dickinson, R., Errico, R., Giorgi, F. and Bates, G. (1989). A regional climate model for the western united states, *Climate Change* .

Dickinson, R., Henderson-Sellers, A. and Kennedy, P. (1993). Biosphere-atmosphere transfer scheme (bats) version 1e as coupled to the ncar community climate model, *Technical report*, National Center for Atmospheric Research.

Dickinson, R., Kennedy, P., Henderson-Sellers, A. and Wilson, M. (1986). Biosphere-atmosphere transfer scheme (bats) for the ncar community climate model, *Technical report*, National Center for Atmospheric Research.

Emanuel, K. A. (1991). A scheme for representing cumulus convection in large-scale models, *Quart. J. Roy. Meteor.Soc.* **48**: 2313–2335.

Fritsch, J. M. and Chappell, C. F. (1980). Numerical prediction of convectively driven mesoscale pressure systems. part i: Convective parameterization, *Journal of Atmospheric Sciences* .

Giorgi, F. (1989). Two-dimensional simulations of possible mesoscale effects of nuclear war fires, *Journal of Geophysical Research* .

Giorgi, F. (1990a). Sensitivity of simulated wintertime precipitation and soil hydrology simulation over the western united states to lower boundary specifications, *Atmos. Ocean* .

Giorgi, F. (1990b). Simulation of regional climate using a limited area model nested in a general circulation model, *Journal of Climate* .

Giorgi, F. (1991). Sensitivity of simulated summertime precipitation over the western united states to different physics parameterization, *Monthly Weather Review* .

Giorgi, F. (1995). Perspectives for regional earth system modeling, *Global Planet Change* .

Giorgi, F. and Bates, G. (1989). The climatological skill of a regional model over complex terrain, *Monthly Weather Review* .

Giorgi, F., Bates, G. and Nieman, S. (1992a). Simulation of the arid climate of the southern great basin using a regional climate model, *Bulletin of the American Meteorological Society* .

Giorgi, F., Bates, G. and Nieman, S. (1993a). The multi-year surface climatology of a regional atmospheric model over the western united states, *Journal of Climate* .

Giorgi, F., Bi, X. and Qian, Y. (2002). Radiative forcing and regional climatic effects of anthropogenic aerosols over east asia: A regional coupled climate-chemistry/aerosols model study, *Journal of Geophysical Research* .

Giorgi, F., Bi, X. and Qian, Y. (2003a). Indirect vs. direct effects of anthropogenic sulfate on the climate of east asia as simulated with a regional coupled climate-chemistry/aerosol model, *Climate Change* .

Giorgi, F., Francisco, R. and Pal, J. (2003b). Effects of a subgrid-scale topography and land use scheme on the simulation of surface climate and hydrology. part 1: Effects of temperature and water vapor disaggregation., *Journal of Hydrometeorology* .

Giorgi, F., Hostetler, S. and Brodeur, C. S. (1994a). Analysis of the surface hydrology in a regional climate model, *Quarterly Journal of the Royal Meteorological Society* .

Giorgi, F., Huang, Y., Nishizawa, K. and Fu, C.-B. (1999). A seasonal cycle simulation over eastern asia and its sensitivity to radiative transfer and surface processes, *Journal of Geophysical Research* .

Giorgi, F. and Marinucci, M. (1991). Validation of a regional atmospheric model over europe: Sensitivity of wintertime and summertime simulations to selected physics parameterizations and lower boundary conditions, *Quarterly Journal of the Royal Meteorological Society* .

Giorgi, F. and Marinucci, M. (1996). An investigation of the sensitivity of simulated precipitation to the model resolution and its implications for climate studies, *Monthly Weather Review* .

Giorgi, F., Marinucci, M. and Bates, G. (1993b). Development of a second generation regional climate model (regcm2) i: Boundary layer and radiative transfer processes, *Monthly Weather Review* .

Giorgi, F., Marinucci, M., Bates, G. and DeCanio, G. (1993c). Development of a second generation regional climate model (regcm2) ii: Convective processes and assimilation of lateral boundary conditions, *Monthly Weather Review* .

Giorgi, F., Marinucci, M. and Visconti, G. (1990). Use of a limited-area model nested in a general circulation model for regional climate simulation over europe, *Journal of Geophysical Research* .

Giorgi, F., Marinucci, R. and Visconti, G. (1992b). 2xco2 climate change scenario over europe generated using a limited area model nested in a general circulation model, 2, *Climate Change Scenario* .

Giorgi, F. and Mearns, L. (1991). Approaches to regional climate change simulation: A review, *Review of Geophysics* .

Giorgi, F. and Mearns, L. O. (1999). Introduction to special section: Regional climate modeling revisited, *Journal of Geophysical Research* .

Giorgi, F., Mearns, L., Shields, C. and L.Mayer (1996). A regional model study of the importance of local versus remote controls of the 1988 drought and the 1993 flood over the central united states, *Journal of Climate* .

Giorgi, F., Mearns, L., Shields, C. and McDaniel, L. (1998). Regional nested model simulations of present day and 2xco2 climate over the central great plains of the united states, *Climate Change* .

Giorgi, F., Shields, C., Brodeur and Bates, G. (1994b). Regional climate change scenarios over the united states produced with a nested regional climate model: Spatial and seasonal characteristics, *Journal of Climate* .

Grell, G. (1993). Prognostic evaluation of assumptions used by cumulus parameterizations, *Monthly Weather Review* .

Grell, G. A., Dudhia, J. and Stauffer, D. R. (1994a). A description of the fifth-generation penn state/ncar mesoscale model (mm5), *Technical report*, National Center for Atmospheric Research.

Grell, G., Dudhia, J. and Stauffer, D. (1994b). A description of the fifth-generation Penn State/NCAR mesoscale model (MM5). Tech. Note TN-398+IA, *Technical report*, National Center for Atmospheric Research.

Grell, G., Kuo, Y.-H. and Pasch, R. J. (1991). Semi-prognostic tests of cumulus parameterization schemes in the middle latitudes, *Monthly Weather Review* .

Hack, J., Boville, B., Briegleb, B., Kiehl, J., Rasch, P. and Williamson, D. (1993). Description of the ncar community climate model (ccm2), *Technical report*, National Center for Atmospheric Research.

Henderson-Sellers, B. (1986). Calculating the surface energy balance for lake and reservoir modeling: A review, *Rev. Geophys.* .

High resolution models of the planetary boundary layer in Advances in Environmental Science and Engineering (1979). Gordon and Breach, Newark, N.J.

Hirakucci, H. and Giorgi, F. (1995). Multiyear present-day and 2xco2 simulations of monsoon-dominated climate over eastern asia and japan with a regional climate model nested in a general circulation model, *Journal of Geophysical Research* .

Holtslag, A. and Boville, B. (1989). Local versus nonlocal boundary-layer diffusion in a global climate model, *Journal of Climate* .

Holtslag, A. and Boville, B. (1993). Local versus nonlocal boundary-layer diffusion in a global climate model, *Journal of Climate* .

Holtslag, A., de Bruijn, E. and Pan, H.-L. (1990). A high resolution air mass transformation model for short-range weather forecasting, *Monthly Weather Review* .

Hostetler, S., Bates, G. and Giorgi, F. (1993). Interactive nesting of a lake thermal model within a regional climate model for climate change studies, *Geophysical Research* .

Hostetler, S., Giorgi, F. and Bates, G. (1994a). Role of lake-atmosphere feedbacks in sustaining lakes bonneville and lahontan 18,000 years ago, *Science* .

Hostetler, S., Giorgi, F., Bates, G. and Bartlein, P. (1994b). Lake-atmosphere feedbacks associated with paleolakes bonneville and lahontan, *Science* .

Hsie, E., Anthes, R. and Keyser, D. (1984). Numerical simulation of frontogenisis in a moist atmosphere, *Journal of Atmospheric Sciences* .

Kato, H., Hirakuchi, H., Nishizawa, K. and Giorgi, F. (1999). Performance of ncar regcm in the simulation of june and january climate over eastern asia and the high-resolution effect of the model, *Journal of Geophysical Research* .

Kiehl, J., Hack, J., Bonan, G., Boville, B., Breigleb, B., Williamson, D. and Rasch, P. (1996). Description of the ncar community climate model (ccm3), *Technical report*, National Center for Atmospheric Research.

Kuo, S.-L. (1974). Further studies of the parameterization of the effect of cumulus convection on large-scale flow, *Journal of Atmospheric Sciences* .

Leung, L., Ghan, S., Zhao, Z.-C., Luo, Y., Wang, W.-C. and Wei, H.-L. (1999). Intercomparison of regional climate simulations of the 1991 summer monsoon in eastern asia, *Journal of Geophysical Research* .

Liu, Y.-Q., Avissar, R. and Giorgi, F. (1996). A simulation with the regional climate model regcm2 of extremely anomalous precipitation during the 1991 east asian flood: An evaluation study, *Journal of Geophysical Research* .

Liu, Y.-Q., Giorgi, F. and Washington, W. (1994). Simulation of summer monsoon climate over east asia with ncar regional climate model, *Monthly Weather Review* .

Marinucci, M. and Giorgi, F. (1992). A 2xco2 climate change scenario over europe generated using a limited area model nested in a general circulation model, i: Present-day climate simulation, *Journal of Geophysical Research* .

Mearns, L., Bogardi, I., Giorgi, F., Matyasovszky, I. and Palecki, M. (1999a). Comparison of climate change scenarios generated from regional climate model experiments and statistical downscaling, *Journal of Geophysical Research* .

Mearns, L., Giorgi, F., McDaniel, L. and Brodeur, C. S. (1995). Analysis of daily variability and diurnal range of temperature in a nested regional climate models: Comparison with observations and doubled co2 results, *Climate Dynamics* .

Mearns, L., Mavromatis, T. and Tsvetsinskaya, E. (1999b). Comparative responses of epic and ceres crop models to high and low spatial resolution climate change scenarios, *Journal of Geophysical Research* .

Pal, J., Small, E. and Eltahir, E. (2000). Simulation of regional-scale water and energy budgets: Representation of subgrid cloud and precipitation processes within regcm, *Journal of Geophysical Research-Atmospheres* .

Pan, Z.-T., Takle, E., Segal, M. and Arritt, R. (1999). Simulation of potential impacts of man-made land use changes on u.s. summer climate under various synoptic regimes, *Journal of Geophysical Research* .

Patterson, J. and Hamblin, P. (1988). Thermal simulation of a lake with winter ice cover, *Limn. Oceanography* .

Perkey, D. and Kreitzberg, C. (1976). A time-dependent lateral boundary scheme for limited -area primitive equation models, *Monthly Weather Review* .

Qian, J.-H., Giorgi, F. and Fox-Rabinovitz, M. (1999). Regional stretched grid generation and its application to the ncar regcm, *Journal of Geophysical Research* .

Qian, Y., Giorgi, F. and Huang, Y. (2001). Regional simulation of anthropogenic sulfur over east asia and its sensitivity to model parameters, *Tellus* .

Seth, A. and Giorgi, F. (1998). The effect of domain choice on summer precipitation simulation and sensitivity in a regional climate model, *Journal of Climate* .

Shea, D., Trenberth, K. and Reynolds, R. (1992). A global monthly sea surface temperature climatology, *Journal of Climate* .

Slingo, J. (1980). A cloud parameterization scheme derived from gate data for use with a numerical model, *Quarterly Journal of the Royal Meteorological Society* .

Slingo, J. (1989). A gcm parameterization for the shortwave radiative properties of water clouds, *Journal of Atmospheric Sciences* .

Small, E., Giorgi, F. and Sloan, L. (1999). Regional climate model simulation of precipitation in central asia: Mean and interannual variability, *Journal of Geophysical Research* .

Small, E. and Sloan, L. (1999). Simulating the water balance of the aral sea with a coupled regional climate-lake model, *Journal of Geophysical Research* .

Sun, L.-Q., Semazzi, F., Giorgi, F. and Ogallo, L. (1999a). Application of the ncar regional climate model to eastern africa, 1. simulation of the short rains of 1988, *Journal of Geophysical Research* .

Sun, L.-Q., Semazzi, F., Giorgi, F. and Ogallo, L. (1999b). Application of the ncar regional climate model to eastern africa, 2. simulation of interannual variability of short rains, *Journal of Geophysical Research* .

Sundqvist, H., Berge, E. and Kristjansson, J. (1989). The effects of domain choice on summer precipitation simulation and sensitivity in a regional climate model, *Journal of Climate* .

Trenberth, K. (1992). Global analyses from ecmwf and atlas of 1000 to 10mb circulation statistics, *Technical report*, National Center for Atmospheric Research.

Zeng, X., Zhao, M. and Dickinson, R. E. (1998). Intercomparison of bulk aerodynamic algoriths for the computation of sea surface fluxes using toga coare and tao data, *Journal of Climate* .

Zhang, D.-L., Hsie, E.-Y. and Moncrieff, M. (1988). A comparison of explicit and implicit predictions of convective and stratiform precipitating weather systems with a meso-β-scale numerical model, **114**: 31–60.

Zhang, G.-J. and McFarlane, N. (1995). Sensitivity of climate simulations to parameterization of cumulus convection in the canadian climate centre general circulation model, *Atmos. Ocean* .